Geosciences Journal
Vol. 16, No. 3, p. 275 − 287, September 2012
DOI 10.1007/s12303-012-0027-2

Demise of an extensive biostromal microbialite in the Furongian (late Cambrian) Chaomidian Formation, Shandong Province, China

Jeong-Hyun Lee
Jitao Chen*
S.K. Chough
School of Earth and Environmental Sciences, Seoul National University, Seoul 151-747, Republic of Korea

ABSTRACT: This study focuses on an extensive biostromal microbialite (10–20 m in thickness and over 6,000 km^2 in area) and the overlying grainstones in the Furongian Chaomidian Formation, Shandong Province, China in order to understand the demise of the microbialite. The microbialites are characterized by centimeter- to decimeter-scale maze-like maceria structures and/or chaotic mesostructures. According to the megastructures of microbialites and the proportion of non-microbial carbonate sediment, the biostromal microbialite is generally divided into the lower and the upper parts, separated by a distinct surface. The lower part is laterally continuous and generally flat-bedded, whereas the upper part shows variable domal megastructures and locally co-occurs with abundant non-microbial carbonate sediment. The entire microbialite bed is sharply overlain by grainstone-dominated deposits via an erosion surface which is either irregular with significant relief or flat with hematitic coating. The lower part of the biostromal microbialites with flat-bedded megastructures most likely deposited contemporaneously during sea-level highstand in the early middle Furongian, as evinced by well-correlated flat-bedded units separated by distinct bounding surfaces. The microbialites formed regional topographic variation, generally deepening toward southeast. The flat-bedded microbialites were drowned by subsequent rapid rise in sea level. In the topographic highs, the microbialites caught up with sea-level rise, forming large-scale domal megastructures. In the topographic lows, however, domal microbialites formed together with abundant non-microbial sediment, which were frequently reworked by storm-induced waves and currents. Subsequent deposition and migration of coarse-grained non-microbial sediment during sea-level rise terminated the entire microbialites.

Key words: biostromal microbialite, rapid sea-level rise, erosion surface, epeiric platform

1. INTRODUCTION

Biostromal microbialites are characterized by approximately flat basal and top surfaces, indicating relatively low topographic relief (Kershaw, 1994). They often formed on carbonate ramps or epeiric platforms during the Cambrian greenhouse period, when continuous rise in eustatic sea level provided favorable conditions for carbonate production and microbial growth (Aitken, 1967; Campbell, 1976; Tucker and Wright, 1990; Kiessling et al., 2002; Rowland and Shapiro, 2002; Lee et al., 2010; Woo and Chough, 2010). Besides, biostromal microbialites were commonly sensitive to the sea-level changes (Tucker, 1977; Southgate, 1989; Adams et al., 2005). They were often terminated by drowning, increased input of clastic sediment, submarine erosion, and subaerial exposure, which are all closely related to sea-level changes (Tucker, 1977; Grotzinger, 1989; Sami and James, 1994; Kershaw et al., 1999; Adams et al., 2005; Grotzinger et al., 2005).

In the North China Platform, microbialites of various types formed in abundance during the Cambrian (Chough et al., 2010). They initiated during the middle Cambrian Series 2 to the early Cambrian Series 3 (Zhushadong and Mantou formations, including microbial laminite, stromatolite, and thrombolite) (Lee and Chough, 2011), and prevailed during the middle-late Cambrian Series 3 (Zhangxia Formation, including *Epiphyton* framestone, thrombolite, dendrolite, and stromatolite) (Woo et al., 2008; Woo, 2009; Howell et al., 2011). The microbialites were terminated by platform drowning in the late Cambrian Series 3, due to rapid rise in relative sea level (Chen et al., 2011). In the middle Furongian, an extensive biostromal microbialite (10–20 m in thickness, >6,000 km^2 in area) formed in the Chaomidian Formation in Shandong Province, which is characterized by centimeter- to decimeter-scale maze-like maceriae structures and/or chaotic mesostructure (Lee et al., 2010). The biostromal microbialite was then demised and replaced by various grainstones, without significant resurgence.

This paper focuses on the demise of the microbialite. Although sea-level rise was important for the abrupt facies shift from microbialites to grainstones (Lee et al., 2010; Chen et al., 2011), there must have been subtle balance among carbonate production, hydrodynamic conditions, and topographic relief. How did sea-level rise affect the growth of the microbialite? Were there local or regional variations in water depth which acted as the limiting factor for the microbialite growth? In these regards, we further delve into the regional variability of microbialite-dominated platform in response to relative sea-level fluctuations.

*Corresponding author: jitaochen@126.com

2. GEOLOGICAL SETTING

The North China Platform was an epeiric sea formed on the stable Sino-Korean Block, an extensive area of ~1,500 km east-west and ~1,000 km north-south (Scotese and McKerrow, 1990; Meyerhoff et al., 1991; Meng et al., 1997) (Fig. 1). The platform comprises mixed siliciclastic-carbonate sediments deposited during the greenhouse period from the Cambrian Series 2 to the Middle Ordovician (Meng et al., 1997). The Cambrian succession in Shandong Province consists of six lithostratigraphic units (Liguan, Zhushadong, Mantou, Zhangxia, Gushan, and Chaomidian formations in ascending order), unconformably overlying Precambrian basement rocks (granitic gneiss or metasedimentary rocks) (Meng et al., 1997; Chough et al., 2010) (Fig. 2).

The Chaomidian Formation (190–260 m thick), overlying the shale-dominated Gushan Formation, consists mainly of carbonate facies which represents various shallow-marine environments (Chen et al., 2011). It formed during the Furongian Series, comprising two local stages of the North China Platform: the Changshanian Stage (*Chuangia*, *Changshania*-*Irvingella*, and *Kaolishania* zones) and the Fengshanian Stage (*Ptychaspis*-*Tsinania*, *Quadraticephalus*, and *Mictosaukia* zones) (Chough et al., 2010) (Fig. 2). The Changshanian-Fengshanian stage boundary lies in a thick grainstone deposit (3–16.5 m in thickness) which overlies an extensive biostromal microbialite in the middle part of the Chaomidian Formation (Figs. 2 and 3).

3. THE MICROBIALITE AND THE OVERLYING GRAINSTONE

Eight outcrop sections were measured in detail (cm scale) (Figs. 1b and 3). Sedimentary facies were identified based on composition, grain size, texture, sedimentary structures, and bed geometry (Tables 1 and 2).

3.1. Microbialite

3.1.1. Description

An extensive biostromal microbialite bed occurs in an interval between the underlying limestone-marlstone alternation and limestone breccia and the overlying grainstones (Fig. 3). It comprises three types of microbialites (classified based on macro- and mesostructures): tabular maceriate microbialite (type 1), columnar maceriate microbialite (type 2), and columnar chaotic microbialite (type 3) (Table 1; Fig. 4) (Lee et al., 2010). Columnar microbialites (types 2 and 3) are prevalent in the western sections (Chengouwan, Fenghuangshan, Tangwangzhai, Wanglaoding, and Laopozhuang sections), whereas tabular maceriate microbialites (type 1) are dominant in the eastern sections (Wanliangyu, Duozhuang, and Jiulongshan sections) (Fig. 3).

In megascale, the biostromal microbialite is largely divided into the lower and the upper parts (Fig. 3), which are characterized by flat-bedded and domal structures, respectively (Figs. 5 and 6). The two parts are separated by a distinct flat surface, which can be recognized by an abrupt

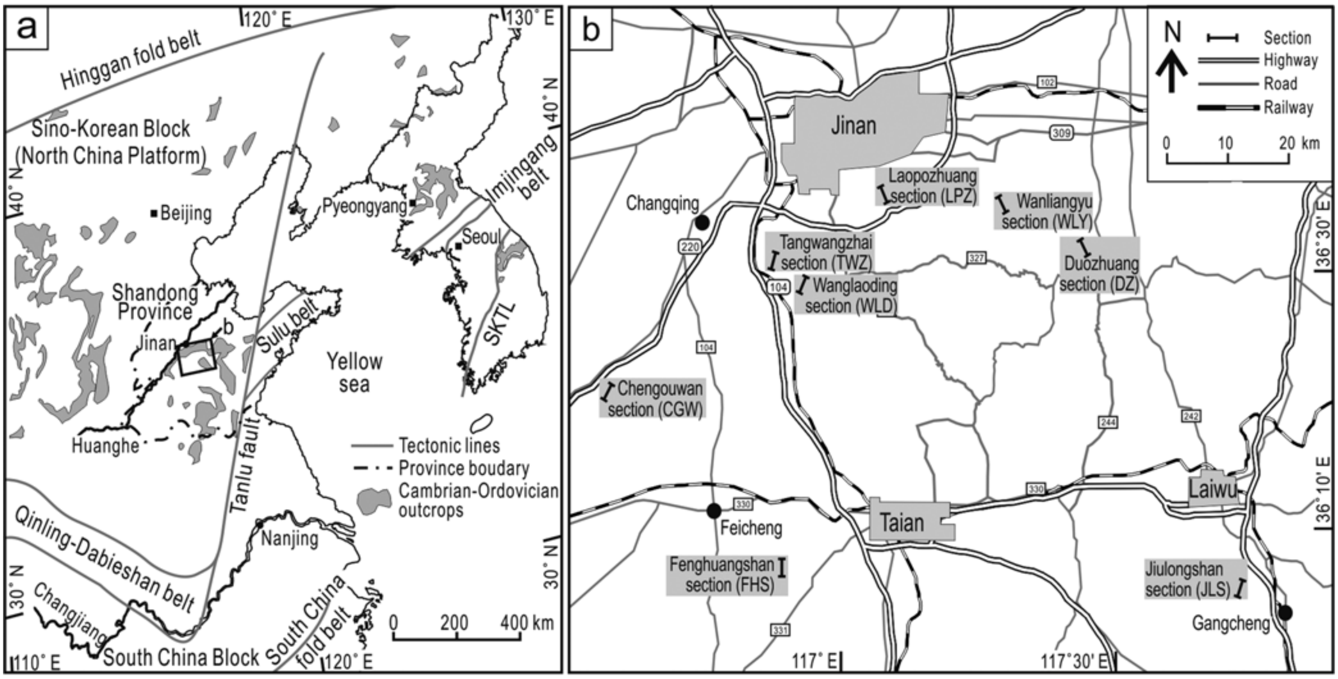

Fig. 1. (a) Distribution of the Cambrian–Ordovician outcrops and major tectonic boundaries of the North China Platform. SKTL: South Korean Tectonic Line (after Kwon et al., 2006). (b) Location map of the measured outcrop sections.

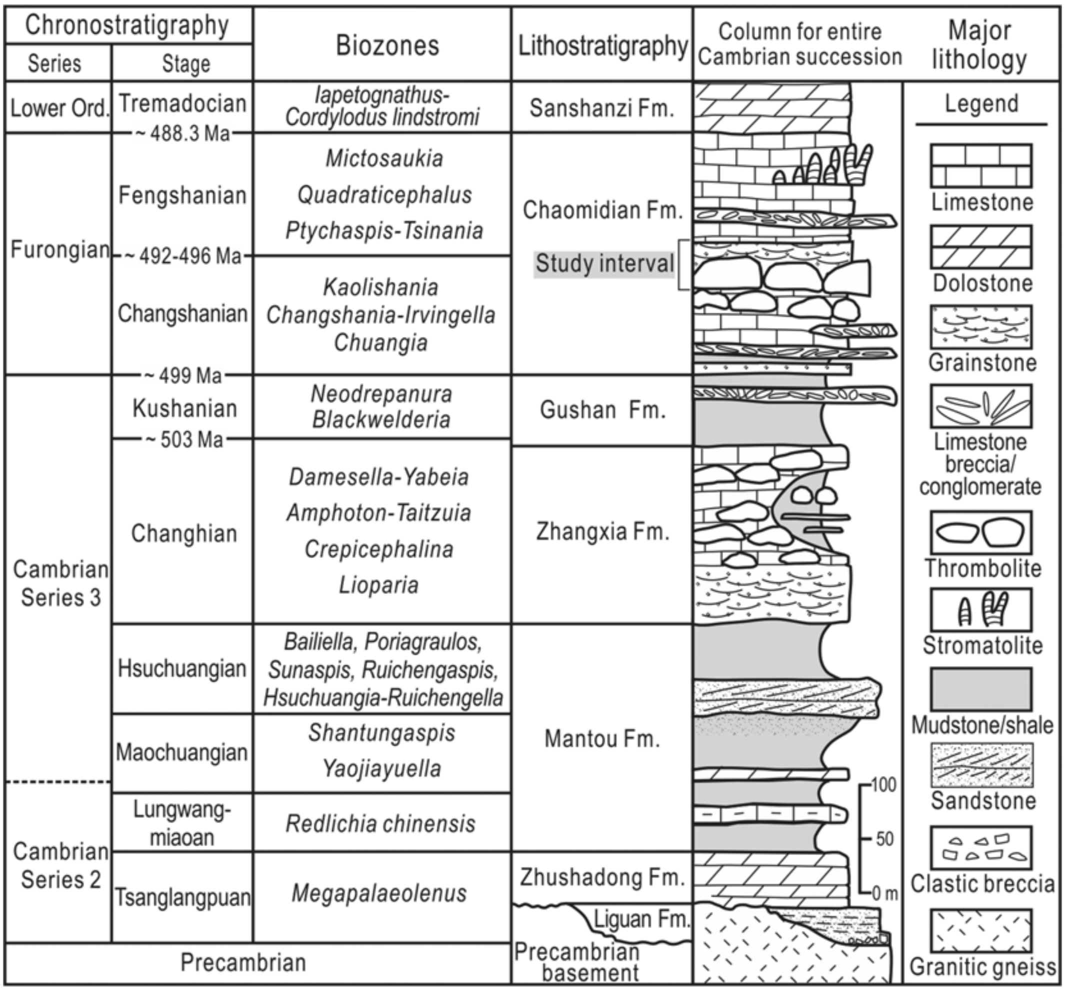

Fig. 2. General biostratigraphy and lithostratigraphy of the Cambrian succession in Shandong Province, China (modified after Chough et al., 2010).

shift in microbialite megastructures, an occurrence of abundant yellowish marlstone within the microbialites directly above the surface, and an occurrence of abundant non-microbial carbonate sediment among the microbialite buildups (Figs. 3, 5, and 6). Both the lower and the upper parts consist of several microbialite beds, which are bounded by either distinct bedding surfaces or non-microbial carbonate sediment (e.g., grainstone, limestone conglomerate, and limestone-marlstone alternation) (Fig. 3).

The lower part of the flat-bedded microbialites consists solely of type 1 microbialite and is generally overlain by non-microbial sediment including limestone-marlstone alternation, limestone conglomerate/breccia, and grainstone (Fig. 3). The middle to upper parts comprise different types of microbialites in the western and eastern sections. Several cyclic units characterized by gradual upward transition from the type 2 to type 3 microbialites occur in the western sections (Figs. 3 and 7), whereas type 1 microbialite occurs dominantly in the eastern sections except for one bed of type 3 microbialite in the Jiulongshan section (Fig. 3). The microbialite units are laterally well traced in the western sections (several to tens of kilometers in distances) and correlated to the eastern sections (Fig. 3).

Domal microbialites are generally convex-up in bed geometry and up to 9 m in thickness (Fig. 5), or laterally discontinuous and associated with abundant grainstone (Figs. 3 and 6). When the domal microbialite laterally co-occurs with grainstone, the margin of microbialite is often erosional (Fig. 6). Generally, types 2 and 3 microbialites are laterally coeval with planar and trough cross-stratified or crudely wavy-stratified bioclastic and oolitic grainstones (Fenghuangshan and Laopozhuang sections) (Fig. 3), whereas type 1 microbialites often with hummocky and swaley cross-stratified peloidal grainstones with small microbialite buildups in between (Wanliangyu and Duozhuang sections) (Fig. 6). The microbialites and co-occurring non-microbial sediment are truncated by an erosional surface (i.e., microbialite-grainstone boundary) which is overlain by various grainstones (Fig. 3).

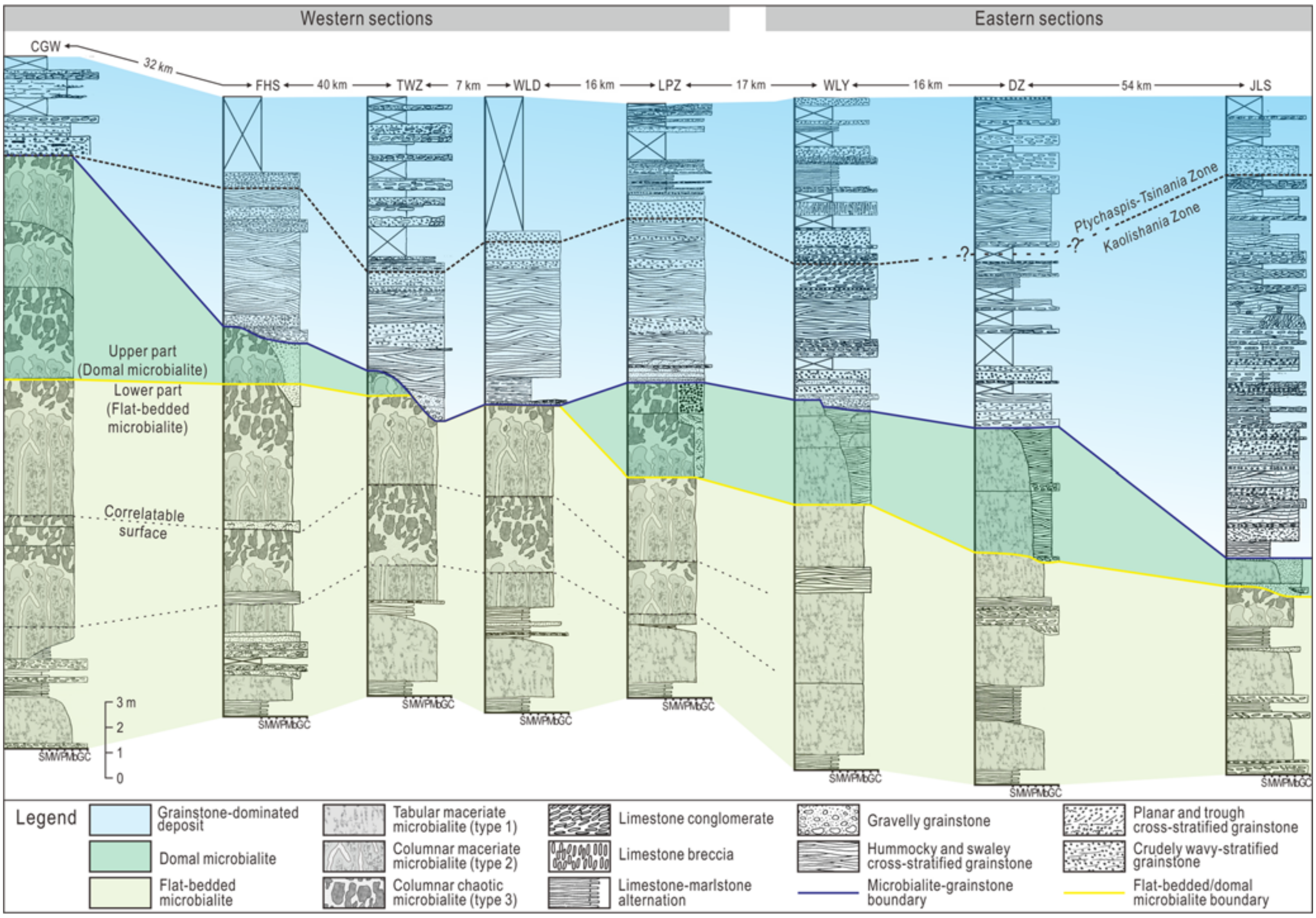

Fig. 3. Detailed sedimentary logs of the biostromal microbialite and the overlying grainstone (for location, see Fig. 1b). The western sections are dominated by columnar microbialites (types 2 and 3), whereas the eastern sections by maceriate microbialites (type 1). The biostromal microbialite is divided into lower (flat-bedded) and upper (domal) parts in megascale, separated by a distinct flat surface. Individual microbialite beds in the western sections are correlated by dotted lines. S: shale, M: mudstone, W: wackestone, P: packstone, Mb: microbialite, G: grainstone, C: conglomerate.

Table 1. Description and interpretation of microbialites (after Lee et al., 2010)

Microbialite types	Macro-structures	Internal structures	Diagram	Description	Interpretation
Tabular maceriate microbialite (type 1)	Tabular	Maceria and chaotic	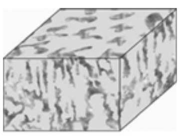	Biohermal/biostromal megastructure (Figs. 4a, b); consists of maceriae and intermacerial sediment with a ragged, obscure boundary; internal structure of maceriae are chaotic (Fig. 4b); intermacerial sediments composed of lime mud and bioclasts; maceriae composed of micrite, *Girvanella*, and *Renalcis*-like microbe.	Low-energy environments below normal wave base.
Columnar maceriate microbialite (type 2)	Columnar	Maceria and chaotic	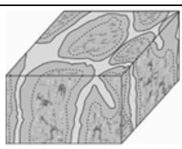	Columnar structure (ca. 60 cm in diameter) within biostrome (Figs. 4c, d); maceriae occur as internal structure, with chaotic outer rim; coarse-grained intercolumnar sediments; type 2 microbialite gradually changes upward to type 3.	Intermediate-energy environments near normal wave base.
Columnar chaotic microbialite (type 3)	Columnar	Chaotic	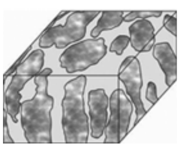	Columnar structure (10–15 cm in diameter) (Figs. 4e, f); elongation ratio of columns ranges from 3:1 to 10:1; smooth, clear boundary; micrite, sparite, peloid, bioclast, *Girvanella* and *Renalcis*-like microbe in microscale; intercolumnar sediments consist of peloids and microbialite clasts of *Girvanella* fragments.	High-energy shallow environments above normal wave base.

Table 2. Description and interpretation of sedimentary facies in the grainstone-dominated deposit

Sedimentary facies	Description	Interpretation
Gravelly grainstone	Massive or normally graded gravelly grainstone (Fig. 8b); composed of bioclasts (trilobites, brachiopods, algae, echinoderms, and cephalopods; a few mm up to 10 mm in length) and peloids (0.2–0.5 mm in diameter); subangular granules and pebbles of lime mudstone or microbialite commonly at base.	Storm-induced lag deposits (Kumar and Sanders, 1976; Kreisa, 1981; Allen, 1982; Kwon and Chough, 2005).
Crudely wavy-stratified grainstone	Crudely wavy-stratified grainstone (Figs. 8e, g); composed of ooids or bioclasts (trilobites, brachiopods, algae, echinoderms, and cephalopods); locally with lime mudstone clasts and glauconite grains; laterally continuous; crudely wavy-stratified, planar and trough cross-stratified; sharp erosional boundaries at base; wave/current ripples locally present.	Deposition in grainstone shoal by waves and currents (Read, 1985; Tucker and Wright, 1990; Osleger, 1991).
Planar and trough cross-stratified grainstone	Planar and/or trough cross-stratified grainstone with angular to tangential contact to the base; partly undulatory bedforms on top surface; composed of ooids or bioclasts (trilobites, brachiopods, echinoderms, and algae).	Subaqueous 2D or 3D dune by currents (Moshier, 1986; Strasser, 1986; Betzler et al., 2007; Palma et al., 2007).
Hummocky and swaley cross-stratified grainstone	Peloidal grainstone, composed of coarse silt- to very fine sand-grade peloids and small fraction of fossil fragments (Fig. 8c); each unit either laterally continuous or discontinuous, varying in thickness from a few cm to 2 m; variation in thickness of laminae.	Storm deposit by combined flow (Allen, 1985; Myrow and Southard, 1996).
Stratified limestone conglomerate	Granule- to pebble-grade, subrounded to rounded lime mudstone clasts (Fig. 8g); bioclastic and peloidal grainstone matrix; mostly matrix-supported and partly clast-supported; normally graded or cross-stratified; often capped by thin ripple cross-stratified peloidal grainstone.	Deposits by strong currents or waves induced by storms (Walker and Plint, 1992; Demicco and Hardie, 1994).
Limestone breccia	Monomictic clasts of laminated or homogeneous lime mudstone; marlstone or peloidal grainstone matrix; clast supported; subrounded to subangular, pebble-grade and flat clasts; partly discontinuous and laterally changing into limestone and marlstone alternation or thin-bedded peloidal grainstone.	Formed by soft-sediment deformation during early diagenesis (Chough et al., 2001; Kwon et al., 2002; Chen et al., 2009a, b).
Limestone and marlstone alternation	Alternation of limestone and marlstone layers; limestone layers about 1–2 cm thick, partly bioturbated, composed of micrite and few bioclasts; marlstone layers about 1–10 mm thick, partly crude laminated, composed of dolomite, calcite, and argillaceous grains.	Deposition in the troughs of submarine dunes (Shinn et al., 1993) or below normal wave base (Pfeil and Read, 1980; Moshier, 1986; Calvet and Tucker, 1988; Keller, 1997).

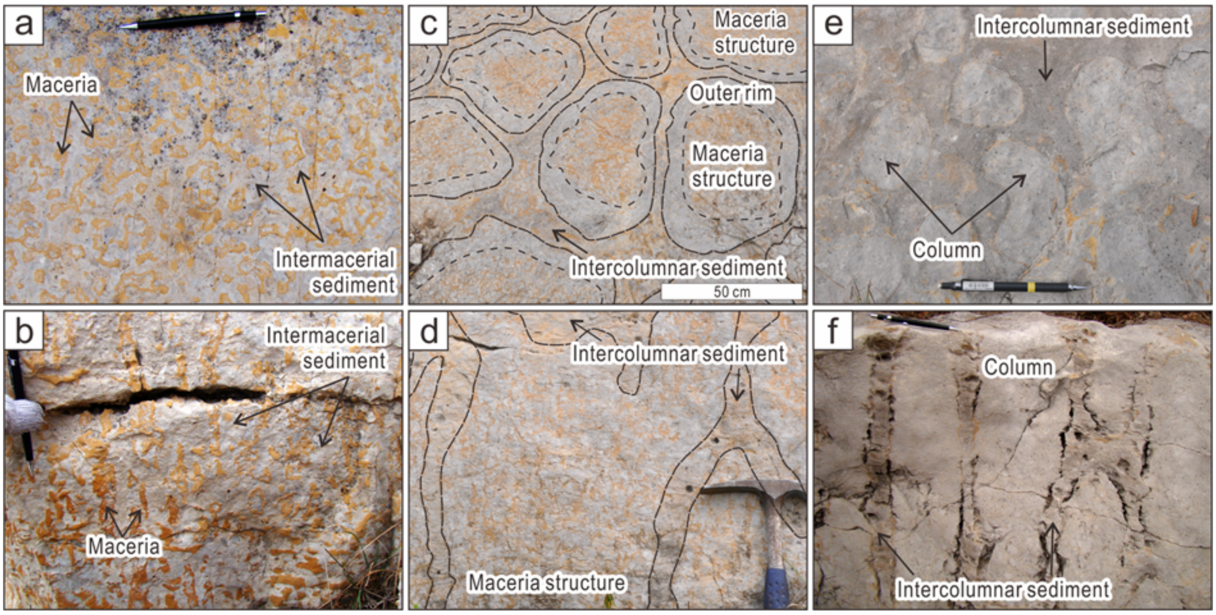

Fig. 4. Three types of microbialites classified based on macro- and mesostructures. (a) Plan view of tabular maceriate microbialite (type 1), with rambling maze-like maceria structures. Pencil in (a), (b), (e), and (f) is 14.5 cm long. (b) Thin ribbon-like maceria structures in the vertical surface of type 1 microbialite. (c) Plan view of columnar maceriate microbialite (type 2), characterized by chaotic outer rim and inner maceria structures. (d) Vertical surface of type 2 microbialite. (e) Plan view of columnar chaotic microbialite (type 3), with intercolumnar space filled with bioclastic grainstone. (f) Vertical surface of type 3 microbialite.

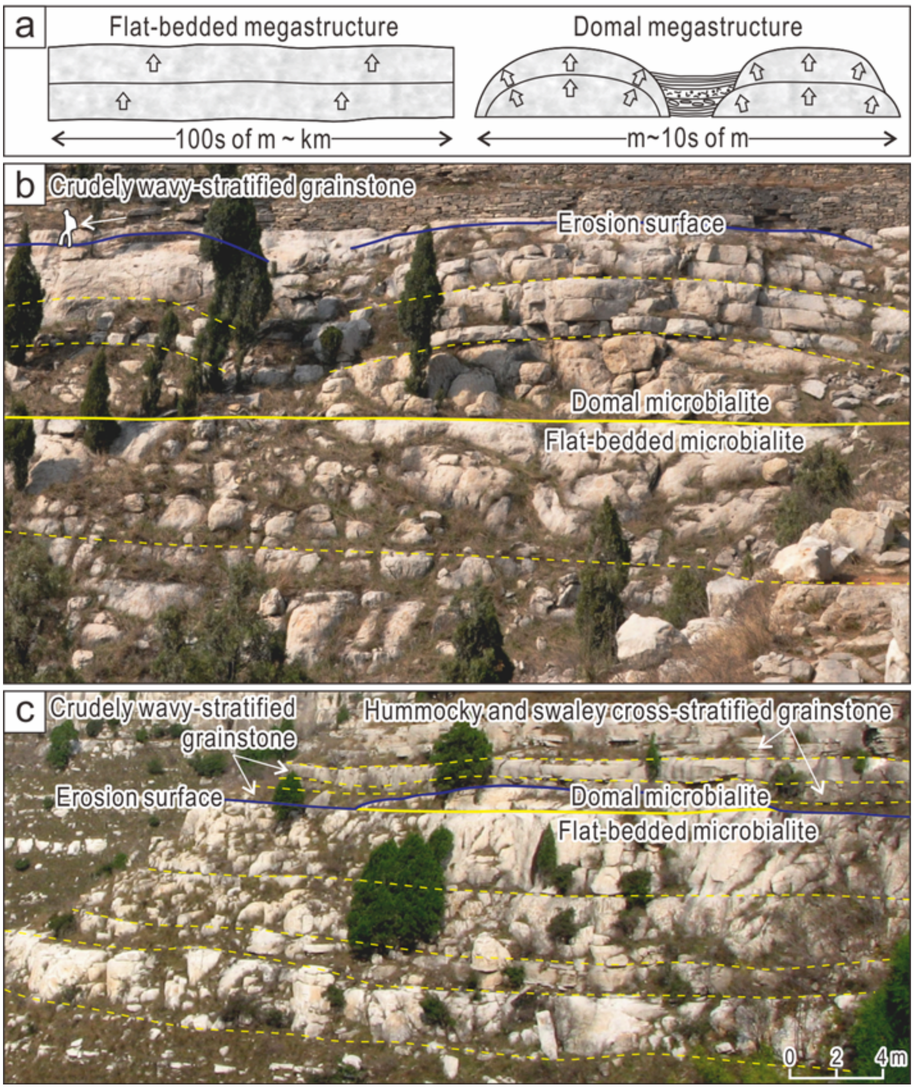

Fig. 5. (a) Terminology for microbialite megastructures. Flat-bedded megastructure is distinctly flat-bedded structure without significant variation in thickness. Non-microbial sediment only constitutes minor portion of this type. Domal megastructure represents curved- or flat-topped structure, laterally co-occurs with non-microbial sediment. Arrows indicate growth direction. (b) Flat-bedded megastructures and domal megastructures of the biostromal microbialite in the Chengouwan section. Arrow in the top left corner points to a sedimentologist for scale. (c) Flat-bedded megastructures and domal megastructures of the biostromal microbialite in the Tangwangzhai section.

3.1.2. Interpretation

The microbialites formed in shallow-water environments with low (type 1), medium (type 2), and high (type 3) energy conditions (Table 1) (Lee et al., 2010). The gradual change from type 2 to 3 microbialites is indicative of upward shallowing water depth and higher energy condition. The distinct bedding surfaces separating the cyclic microbialite units resulted from non-deposition or erosion, most likely accompanied with high-frequency changes in base level. The ubiquitous occurrence of type 1 microbialite at the base of the flat-bedded microbialite and the occurrence of correlatable cyclic microbialite units of type 2 to 3 microbialites in the middle to upper parts collectively indicate contemporaneous development of the microbialite. On the other hand, the occurrence of different types of microbialites in the middle to upper parts of the flat-bedded microbialite indicate that the western sections developed in relatively shallow environments, whereas the eastern sections deposited under relatively deeper environments (Lee et al., 2010).

The entire flat-bedded microbialites most likely formed during sea-level highstand, when the potential growth rate of microbialites exceeded the rate of accommodation production. Microbialites kept up with the slow sea-level rise and filled up the available accommodation, forming flat-bedded megastructures on the extensive paleoseafloor (cf. Southgate, 1989; Sami and James, 1994). Domal microbialites in the upper part formed during rapid rise in sea level, when the rate of sea-level rise was slightly higher than the potential growth rate of microbialites and the sea level did not act as limiting factor for vertical expansion (Grotzinger, 1989; Southgate, 1989; Turner et al., 1997; Lemon, 2000). Domal microbialites also formed when the contemporaneous deposition of large amounts of non-microbial carbonate sediment limited the lateral expansion of microbialites. Therefore, the distinct surface between the underlying flat-bedded microbialites and the overlying domal microbialites is indicative of rapid rise in relative sea level, which is also evinced

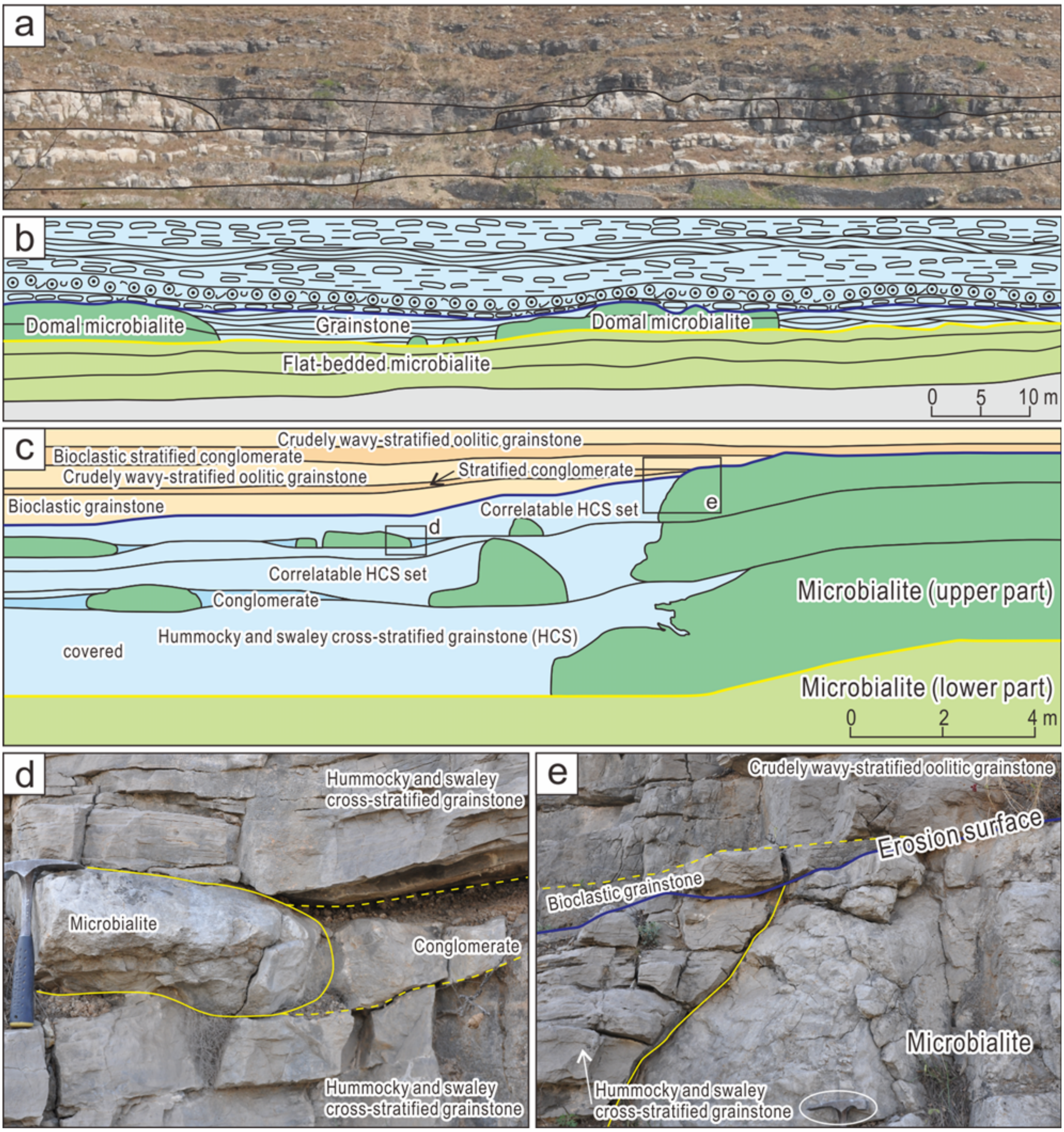

Fig. 6. Outcrop photograph (a) and line drawing (b) of the Duozhuang section, showing the flat-bedded microbialites and overlying domal microbialites which laterally co-occur with hummocky and swaley cross-stratified grainstone. The domal microbialites and the associated sediment are bounded at top by a sharp erosion surface. (c) Line drawing of the upper part of the biostromal microbialite in the Wanliangyu section. The biostromal microbialite laterally changes into hummocky and swaley cross-stratified grainstone, which contains several small microbialite buildups (~1.5 m in height, ~3 m in width). The upper part of the biostromal microbialite and the hummocky and swaley cross-stratified grainstone are both truncated by crudely wavy-stratified grainstone. (d) Small microbialite buildup within hummocky and swaley cross-stratified grainstone, laterally changing into conglomerate. Hammer is 28 cm long. (e) Microbialite and laterally co-occurring hummocky and swaley cross-stratified grainstone are overlain by bioclastic grainstone and crudely wavy-stratified grainstone via a sharp erosion surface. Hammer head is 17 cm long.

by the occurrence of abundant dolomitic marlstone at the base of domal microbialites in the western sections, the occurrence of abundant non-microbial carbonate sediment between microbialite buildups in the eastern sections, and the abrupt change from type 3 to type 1 microbialite in the Jiulongshan section.

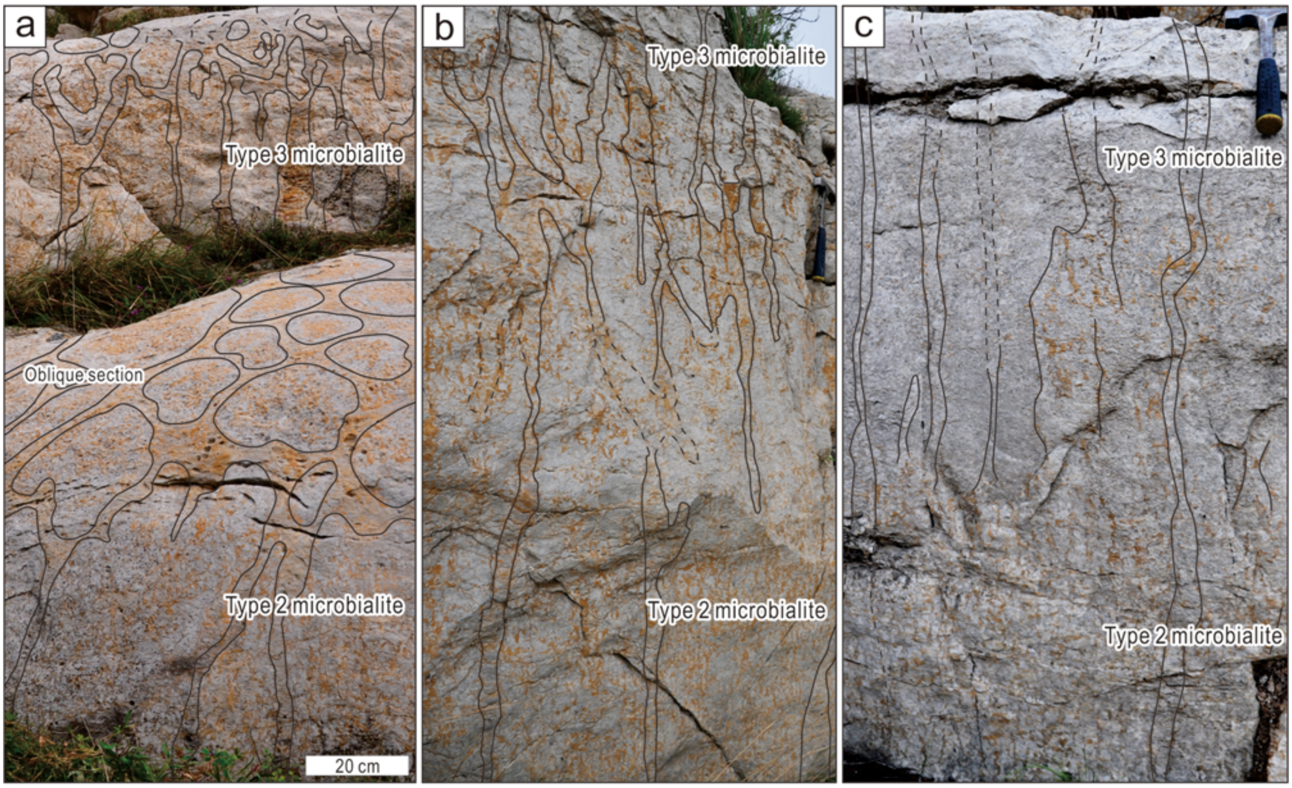

Fig. 7. Gradual changes from type 2 to type 3 microbialites in the western sections. (a) Chengouwan section. (b) Tangwangzhai section. Hammer is 28 cm long. (c) Laopozhuang section.

3.2. Microbialite-Grainstone Boundary

3.2.1. Description

The extensive microbialite is sharply overlain by a grainstone-dominated succession of various thickness (3–16.5 m) with a distinct erosion surface (Figs. 3 and 8). The erosion surface truncates the topmost part of the entire microbialite and the associated sediment between the domal microbialite mounds (Figs. 3, 6, and 8). It is either concave-upward with erosion relief of a few cm to 2 m (Figs. 8a, d, g), or flat locally with hematitic coating (Figs. 8e, f). The erosion surface is usually irregular in the western section (Figs. 8a, d, g) and flat to undulatory in the eastern sections (Fig. 6). Above the irregular surfaces, large clasts (up to 10 cm in diameter) derived from underlying microbialites often occur in the local depressions of the erosion surface, forming normally graded gravelly grainstone or stratified limestone conglomerate (Figs. 8b, g). The entire biostromal microbialite and microbialite-clast-bearing deposit are usually overlain by crudely wavy-stratified or cross-stratified grainstones via a flat erosion surface (Figs. 8e, g). In some cases, the distinct surface (i.e., microbialite-grainstone boundary) is directly overlain by hummocky cross-stratified grainstone or thin-bedded limestone and marlstone alternation (Figs. 8c, d).

3.2.2. Interpretation

The sharp erosion surface was most likely generated by constant submarine erosion under shallow-water, high-energy environments rather than subaerial erosion (Caron et al., 2004), which is implied by complete absence of significant hiatuses or subaerial exposure features (e.g., paleokarst, paleosols, evaporates, and meteoric cementation signatures) (cf. Lee et al., 2010; Chen et al., 2011). The stratified conglomerate and gravelly grainstone with microbialite clasts in the local depressions accumulated as lag deposits during the erosional processes probably caused by storms (Kumar and Sanders, 1976; Kreisa, 1981; Allen, 1982; Kwon and Chough, 2005). The microbialite-grainstone boundary is further modified by constant wave abrasion, forming the flat erosion surface that truncated both the microbialites and the lag deposits (Brett and Brookfield, 1984; Myrow et al., 1999).

3.3. Grainstone Deposit

3.3.1. Description

The grainstone deposit mainly consists of gravelly grainstone, crudely wavy-stratified grainstone, planar and trough cross-stratified grainstone, hummocky and swaley cross-stratified grainstone, limestone and marlstone alternation, limestone conglomerate, and limestone breccia (Table 2),

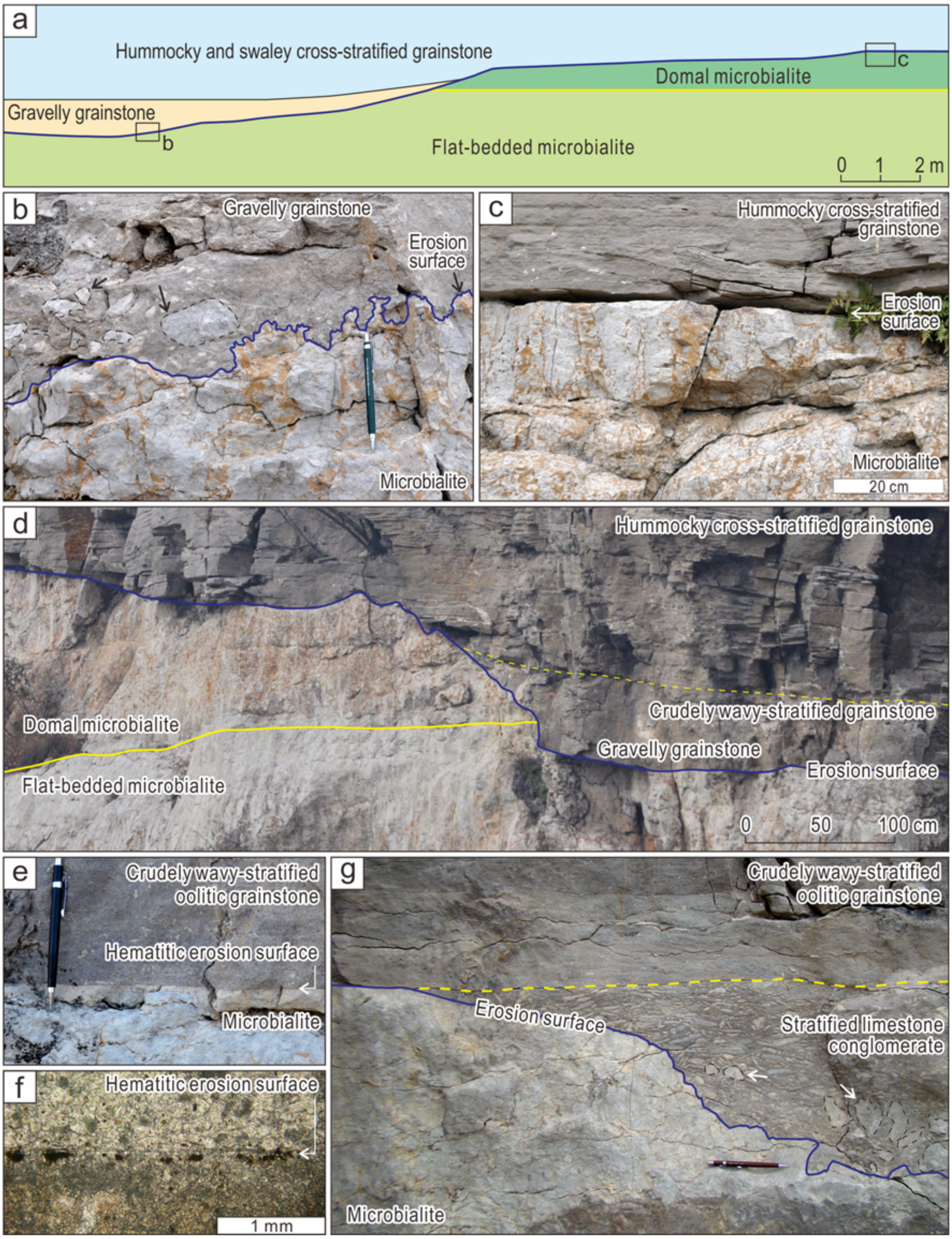

Fig. 8. Sharp erosion surface between the microbialite and the grainstone deposit. (a) Line drawing of the microbialite and the overlying grainstone in the Tangwangzhai section. The gravelly grainstone occurs in the depression of the erosion surface, and hummocky and swaley grainstone overlies both the gravelly grainstone and the microbialite. (b) Gravelly grainstone containing microbialite clasts (arrows) of various sizes overlies the type 3 microbialite with an irregular surface. Pencil is 14.5 cm long. (c) Hummocky and swaley cross-stratified grainstone directly overlies the type 3 microbialite. (d) The microbialite and overlying grainstone are separated by a concave-upward erosion surface (Tangwangzhai section). The gravelly grainstone occurs in the depression. (e) The microbialite is sharply cut by a flat erosion surface, with hematitic coating (Fenghuangshan section). (f) Photomicrograph of the erosion surface with hematitic coating (Wanglaoding section). (g) The microbialite is truncated by an irregular erosion surface (Fenghuangshan section). Large microbialite clasts (arrows) occur within stratified limestone conglomerate. A flat erosion surface (yellow dotted line) truncates both microbialite and conglomerate.

which is generally overlain by a shale-dominated succession (Fig. 3) (Chen et al., 2011). The grainstone deposit shows a general thinning trend from the east to the west (Fig. 3). The lower part of the grainstone deposit is dominated by crudely wavy-stratified or planar and trough cross-stratified, oolitic or bioclastic grainstone which is locally underlain by gravelly grainstone and stratified limestone conglomerate (Figs. 3 and 8d, g). The middle and upper parts of the grainstone deposit is dominated by thick beds (~5 m) of hummocky and swaley cross-stratified peloidal grainstone, which is intercalated with limestone and marlstone, crudely wavy-stratified grainstone, stratified limestone conglomerate, and limestone breccia (Fig. 3). The *Ptychaspis*-*Tsinania* Zone, of which the lower boundary represents Changshanian-Fengshanian stage boundary, occurs in the upper part of the grainstone deposit (Fig. 3).

3.3.2. Interpretation

The crudely wavy-stratified and cross-stratified grainstone in the lower part of the grainstone deposit indicates high-energy, shallow-water environments above normal wave base (Read, 1985; Tucker and Wright, 1990; Osleger, 1991; Nichols, 2009). The hummocky and swaley cross-stratified grainstone indicates storm deposit below normal wave base (Allen, 1985; Myrow and Southard, 1996), whereas intercalated limestone and marlstone alternation indicates low-energy deposition between storm events (Shinn et al., 1993) or below normal wave base (Pfeil and Read, 1980; Moshier, 1986; Calvet and Tucker, 1988; Keller, 1997). The overlying shale-dominated succession suggests submergence of the carbonate shoreface below the storm wave base (Markello and Read, 1981; Osleger and Read, 1991; Chen et al., 2011).

4. DISCUSSION

During sea-level highstand in the early middle Furongian, an extensive microbialite biostrome with flat-bedded megastructures formed on the extensive seafloor of the North China Platform (Fig. 9a). The dominance of different types of microbialites (type 1 vs. types 2 and 3) in different localities of the platform is indicative of topographic variations, with a general southeastward-deepening trend (Fig. 9a). With subsequent rapid rise in sea level, the flat-bedded microbialites were drowned, forming a distinct surface (Fig. 9b). Under deepened waters, domal microbialites deposited as a result of catch-up growth above the flat-bedded microbialites together with abundant input of non-microbial carbonate sediment. During continued rise in sea level, microbialites kept up with sea-level rise in the topographic highs (e.g., Chengouwan section) and formed large-scale domal mega-

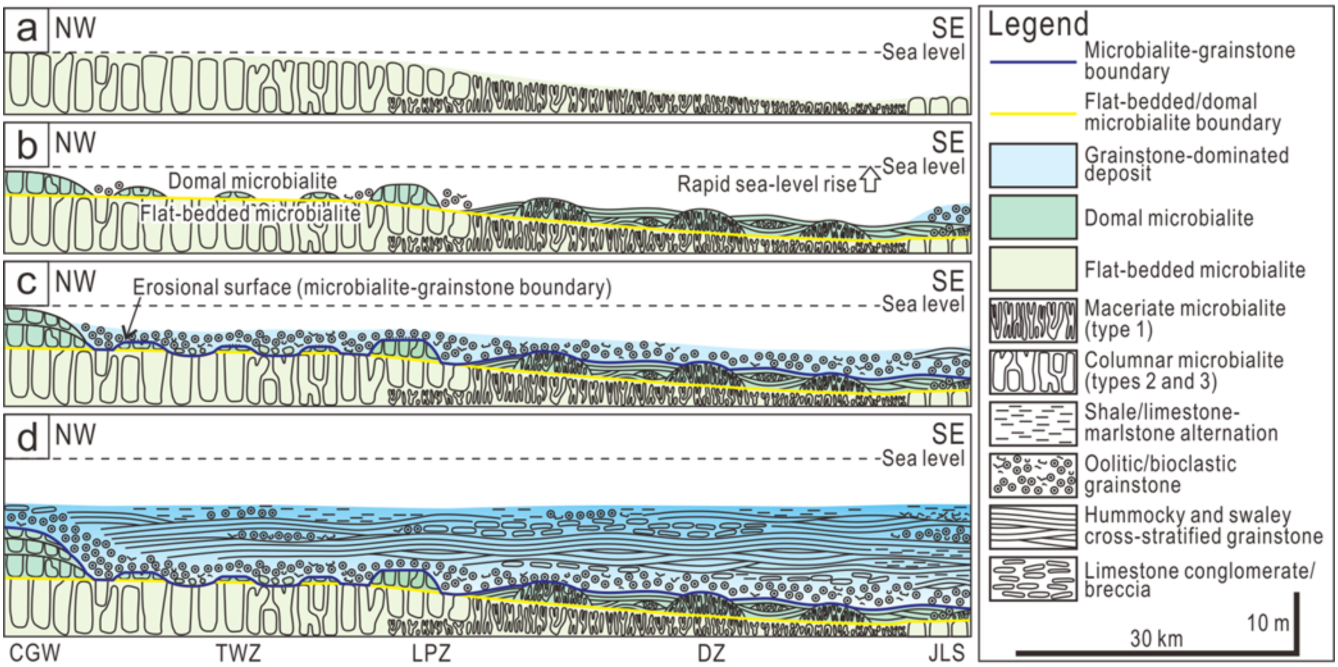

Fig. 9. Depositional model. (a) Flat-bedded microbialites formed contemporaneously on the extensive paleoseafloor during highstand in sea level. Local topographic variation was indicated by different microbialite types; microbialites in the northwest (types 2 and 3) were shallower, whereas those in the southeast (type 1) were deeper. (b) During ensued rapid rise in sea level, laterally discontinuous domal microbialites deposited above the flat-bedded microbialites with contemporaneous deposition of non-microbial sediment under deepened water. (c) While microbialites in topographic highs kept with sea-level rise, those in the topographic lows were eroded by strong storm-induced waves and currents, and terminated by deposition of grainstone. (d) With continued rise in sea level, the microbialites were completely terminated and could not resurge due to increased water depth and input of non-microbial carbonate sediment. For location and full name of the sections, see Figure 1b.

structures (Fig. 9c). In the topographic lows, however, microbialites were subsequently eroded by storm-induced currents and waves, and terminated by deposition of grainstone (Fig. 9c). The microbial carbonate factory was finally demised when the last microbialite (Chengouwan section) was terminated by northwestward migration of grainstone (Fig. 9d). As water deepened continuously, the platform was largely submerged below storm wave base, which resulted in deposition of a shale-dominated succession (Fig. 3).

The biostratigraphic correlation (*Ptychaspis*-*Tsinania* Zone) among sections together with different thickness of the grainstone deposit indicates that the microbialites terminated diachronously, from southeast to northwest (Fig. 3). The significant erosion surface between the biostromal microbialite and the grainstone deposit (e.g., microbialite-bearing gravelly grainstone and hummocky and swaley cross-stratified grainstone) suggest that the demise of microbialite was most likely related to storm processes (e.g., strong erosion, increased turbidity, and burial by input of abundant sediment). The storm-induced processes alone, however, cannot easily terminate the microbialites, as microbialites can survive repetitive storm-induced burial and exposure events (Dibenedetto and Grotzinger, 2005; Bowlin et al., 2012). The termination event must have been accompanied by rapid rise in sea level and subsequent deposition of excessive carbonate sediment produced *in situ* or transported from ambient environments by storm-induced currents. Growth of microbialites would have been limited by increase in water depth, and failed to catch up the rising sea level in the topographic lows (Southgate, 1989; Sami and James, 1994; Kershaw et al., 1999; Adams et al., 2005).

As microbialite growth ceased and abundant carbonate grains were deposited, the transition from microbialite-dominated to grainstone-dominated environments occurred consequently. The grainstone shoal firstly established in relatively deeper environments (e.g., shoreface) where constant reworking of waves and currents was not dampened by friction of the shallow seafloor. The grainstone shoal migrated and deposited in response to both strong hydrodynamic conditions and relative sea-level rise, which progressively terminated the microbialites in the topographic highs. Resurgence of microbialites after the termination was suppressed most likely because of the prolonged unfavorable conditions.

5. CONCLUSIONS

An extensive biostromal microbialite with flat-bedded megastructures formed on the North China epeiric platform during sea-level highstand in the early middle Furongian. With rapid rise in sea level, flat-bedded microbialites were drowned and terminated, forming a distinct surface. During continued rise in sea level, domal microbialites caught up with the sea-level rise in the topographic highs, but failed in the topographic lows. The microbialites were severely eroded by storm-induced waves and currents accompanied by rapid rise in sea level, and progressively terminated by deposition of excessive grainstone. Increased water depth, storm-induced erosion, and subsequent deposition of grainstone collectively inhibited resurgence of microbialites.

ACKNOWLEDGMENTS: This study was supported to SKC by the National Research Foundation of Korea (2011-0030964) and the BK 21 project of Korea (Ministry of Education and Human Resources). We are grateful to Z. Han (Shandong University of Science and Technology) for the logistic support during the field work and the financial support by the National Natural Science Foundation of China (40972043). We thank J. Woo (Korea Polar Research Institute) and S.-J. Choh (Korea University) for carefully reading the earlier version of the manuscript.

REFERENCES

Adams, E.W., Grotzinger, J.P., Watters, W.A., Schröder, S., McCormick, D.S., and Al-Siyabi, H.A., 2005, Digital characterization of thrombolite-stromatolite reef distribution in a carbonate ramp system (terminal Proterozoic, Nama Group, Namibia). AAPG Bulletin, 89, 1293–1318.

Aitken, J.D., 1967, Classification and environmental significance of cryptalgal limestones and dolomites, with illustrations from the Cambrian and Ordovician of southwestern Alberta. Journal of Sedimentary Petrology, 37, 1163–1178.

Allen, J.R.L., 1982, Sedimentary Structures: Their Character and Physical Basis. Elsevier, Amsterdam, 663 p.

Allen, P.A., 1985, Hummocky cross-stratification is not produced purely under progressive gravity waves. Nature, 313, 562–564.

Betzler, C., Pawellek, T., Abdullah, M., and Kossler, A., 2007, Facies and stratigraphic architecture of the Korallenoolith Formation in North Germany (Lauensteiner Pass, Ith Mountains). Sedimentary Geology, 194, 61–75.

Bowlin, E.M., Klaus, J.S., Foster, J.S., Andres, M.S., Custals, L., and Reid, R.P., 2012, Environmental controls on microbial community cycling in modern marine stromatolites. Sedimentary Geology, 263–264, 45–55.

Brett, C.E. and Brookfield, M.E., 1984, Morphology, faunas and genesis of Ordovician hardgrounds from southern Ontario, Canada. Palaeogeography, Palaeoclimatology, Palaeoecology, 46, 233–290.

Calvet, F. and Tucker, M.E., 1988, Outer ramp cycles in the Upper Muschelkalk of the Catalan Basin, northeast Spain. Sedimentary Geology, 57, 185–198.

Campbell, J.A., 1976, Upper Cambrian stromatolitic biostrome, Clinetop Member of the Dotsero Formation, western Colorado. Geological Society of America Bulletin, 87, 13–31.

Caron, V., Nelson, C.S., and Kamp, P.J.J., 2004, Transgressive surfaces of erosion as sequence boundary markers in cool-water shelf carbonates. Sedimentary Geology, 164, 179–189.

Chen, J., Chough, S.K., Chun, S.S., and Han, Z., 2009a, Limestone pseudoconglomerates in the Late Cambrian Gushan and Chaomidian Formations (Shandong Province, China): soft-sediment deformation induced by storm-wave loading. Sedimentology, 56, 1174–1195.

Chen, J., van Loon, A.J., Han, Z., and Chough, S.K., 2009b, Funnel-shaped, breccia-filled clastic dykes in the Late Cambrian Chaomidian Formation (Shandong Province, China). Sedimentary Geology, 221, 1–6.

Chen, J., Chough, S.K., Han, Z., and Lee, J.-H., 2011, An extensive erosion surface of a strongly deformed limestone bed in the Gushan and Chaomidian formations (late Middle Cambrian to Furongian), Shandong Province, China: Sequence–stratigraphic implications. Sedimentary Geology, 233, 129–149.

Chough, S.K., Kwon, Y.K., Choi, D.K., and Lee, D.J., 2001, Autoconglomeration of limestone. Geosciences Journal, 5, 159–164.

Chough, S.K., Lee, H.S., Woo, J., Chen, J., Choi, D.K., Lee, S.-b., Kang, I., Park, T.-Y., and Han, Z., 2010, Cambrian stratigraphy of the North China Platform: revisiting principal sections in Shandong Province, China. Geosciences Journal, 14, 235–268.

Demicco, R.V. and Hardie, L.A., 1994, Sedimentary structures and early diagenetic features of shallow marine carbonates. SEPM, Tulsa, 265 p.

Dibenedetto, S. and Grotzinger, J., 2005, Geomorphic evolution of a storm-dominated carbonate ramp (c. 549 Ma), Nama Group, Namibia. Geological Magazine, 142, 583–604.

Grotzinger, J.P., 1989, Facies and evolution of Precambrian carbonate depositional systems: emergence of the modern platform archetype. In: Crevello, P.D., Wilson, J.L., Sarg, J.F., and Read, J.F. (eds.), Controls on Carbonate Platforms and Basin Development. SEPM, Tulsa, 79–106.

Grotzinger, J.P., Adams, E.W., and Schröder, S., 2005, Microbial–metazoan reefs of the terminal Proterozoic Nama Group (c. 550–543 Ma), Namibia. Geological Magazine, 142, 499–517.

Howell, J., Woo, J., and Chough, S.K., 2011, Dendroid morphology and growth patterns: 3-D computed tomographic reconstruction. Palaeogeography, Palaeoclimatology, Palaeoecology, 299, 335–347.

Keller, M., 1997, Evolution and sequence stratigraphy of an Early Devonian carbonate ramp, Cantabrian Mountains, northern Spain. Journal of Sedimentary Research, 67, 638–652.

Kershaw, S., 1994, Classification and Geological Significance of Biostromes. Facies, 31, 81–92.

Kershaw, S., Zhang, T.S., and Lan, G.Z., 1999, A ?microbialite carbonate crust at the Permian-Triassic boundary in South China, and its palaeoenvironmental significance. Palaeogeography, Palaeoclimatology, Palaeoecology, 146, 1–18.

Kiessling, W., Flügel, E., and Golonka, J., 2002, Phanerozoic Reef Patterns. SEPM, Tulsa, 775 p.

Kreisa, R.D., 1981, Storm-generated sedimentary structures in subtidal marine facies with examples from the Middle and Upper Ordovician of Southwestern Virginia. Journal of Sedimentary Petrology, 51, 823–848.

Kumar, N. and Sanders, J.E., 1976, Characteristics of shoreface storm deposits: modern and ancient examples. Journal of Sedimentary Petrology, 46, 145–162.

Kwon, Y.K., Chough, S.K., Choi, D.K., and Lee, D.J., 2002, Origin of limestone conglomerates in the Choson Supergroup (Cambro-Ordovician), mid-east Korea. Sedimentary Geology, 146, 265–283.

Kwon, Y.K. and Chough, S.K., 2005, Sequence stratigraphy of the cyclic successions in the Dumugol Formation (Lower Ordovician), mideast Korea. Geosciences Journal, 9, 305–324.

Kwon, Y.K., Chough, S.K., Choi, D.K., and Lee, D.J., 2006, Sequence stratigraphy of the Taebaek Group (Cambrian-Ordovician), mideast Korea. Sedimentary Geology, 192, 19–55.

Lee, H.S. and Chough, S.K., 2011, Depositional processes of the Zhushadong and Mantou formations (Early to Middle Cambrian), Shandong Province, China: roles of archipelago and mixed carbonate-siliciclastic sedimentation on cycle genesis during initial flooding of the North China Platform. Sedimentology, 58, 1530–1572.

Lee, J.-H., Chen, J., and Chough, S.K., 2010, Paleoenvironmental implications of an extensive maceriate microbialite bed in the Furongian Chaomidian Formation, Shandong Province, China. Palaeogeography, Palaeoclimatology, Palaeoecology, 297, 621–632.

Lemon, N.M., 2000, Neoproterozoic fringing stromatolite reef complex, Flinders Ranges, South Australia. Precambrian Research, 100, 109–120.

Markello, J.R. and Read, J.F., 1981, Carbonate ramp-to-deeper shale shelf transitions of an Upper Cambrian intrashelf basin, Nolichucky Formation, Southwest Virginia Appalachians. Sedimentology, 28, 573–597.

Meng, X., Ge, M., and Tucker, M.E., 1997, Sequence Sequence stratigraphy, sea-level changes and depositional systems in the Cambro-Ordovician of the North China carbonate platform. Sedimentary Geology, 114, 189–222.

Meyerhoff, A.A., Kamen-Kaye, M., Chen, C., and Taner, I., 1991, China - Stratigraphy, Paleogeography, and Tectonics. Kluwer Academic Publishers, Dordrecht, Netherlands, 188 p.

Moshier, S.O., 1986, Carbonate Platform Sedimentology, Upper Cambrian Richland Formation, Lebanon Valley, Pennsylvania. Journal of Sedimentary Petrology, 56, 204–216.

Myrow, P.M. and Southard, J.B., 1996, Tempestite deposition. Journal of Sedimentary Research, 66, 875–887.

Myrow, P.M., Taylor, J.F., Miller, J.F., Ethington, R.L., Ripperdan, R.L., and Brachle, C.M., 1999, Stratigraphy, sedimentology, and paleontology of the Cambrian-Ordovician of Colorado. In: Lageson, D.R., Lester, A.P., and Trudgill, B.D. (eds.), Colorado and Adjacent Areas. Geological Society of America, Boulder, 157–176.

Nichols, G., 2009, Sedimentology and Stratigraphy (2nd edition). Wiley-Blackwell, Oxford, 419 p.

Osleger, D., 1991, Subtidal carbonate cycles: Implications for allocyclic vs. autocyclic controls. Geology, 19, 917–920.

Osleger, D. and Read, J.F., 1991, Relation of eustasy to stacking patterns of meter-scale carbonate cycles, Late Cambrian, USA. Journal of Sedimentary Petrology, 61, 1225–1252.

Palma, R.M., López-Gómez, J., and Piethé, R.D., 2007, Oxfordian ramp system (La Manga Formation) in the Bardas Blancas area (Mendoza Province) Neuquén Basin, Argentina: Facies and depositional sequences. Sedimentary Geology, 195, 113–134.

Pfeil, R.W. and Read, J.F., 1980, Cambrian carbonate platform margin facies, Shady Dolomite, southwestern Virginia, U.S.A. Journal of Sedimentary Petrology, 50, 91–116.

Read, J.F., 1985, Carbonate platform facies models. AAPG Bulletin, 69, 1–21.

Rowland, S. and Shapiro, R.S., 2002, Reef patterns and environmental influences in the Cambrian and earliest Ordovician. In: Kiessling, W., Flügel, E., and Golonka, J. (eds.), Phanerozoic Reef Patterns. SEPM, Tulsa, 95–128.

Sami, T.T. and James, N.P., 1994, Peritidal carbonate platform growth and cyclicity in an early Proterozoic foreland basin, Upper Pethei Group, northwest Canada. Journal of Sedimentary Research, B64, 111–131.

Scotese, C.R. and McKerrow, W.S., 1990, Revised world maps and introduction. In: McKerrow, W.S. and Scotese, C.R. (eds.), Palaeozoic Palaeogeography and Biogeography. Geological Society, 1–

21.
Shinn, E.A., Steinen, R.P., Dill, R.F., and Major, R., 1993, Lime-mud layers in high-energy tidal channels: A record of hurricane deposition. Geology, 21, 603–606.
Southgate, P.N., 1989, Relationships between cyclicity and stromatolite form in the Late Proterozoic Bitter Springs Formation, Australia. Sedimentology, 36, 323–339.
Strasser, A., 1986, Ooids in Purbeck limestones (lowermost Cretaceous) of the Swiss and French Jura. Sedimentology, 33, 711–727.
Tucker, M.E., 1977, Stromatolite biostromes and associated facies in the late Precambrian porsanger dolomite formation of Finnmark, Arctic Norway. Palaeogeography, Palaeoclimatology, Palaeoecology, 21, 55–83.
Tucker, M.E. and Wright, V.P., 1990, Carbonate Sedimentology. Blackwell, Oxford, 482 p.
Turner, E.C., James, N.P., and Narbonne, G.M., 1997, Growth dynamics of Neoproterozoic calcimicrobial reefs, Mackenzie Mountains, Northwest Canada. Journal of Sedimentary Research, 67, 437–450.
Walker, R.G. and Plint, A., 1992, Wave- and storm-dominated shallow marine systems. In: Walker, R.G. and James, N.P. (eds.), Facies Models: Response to Sea Level Change. Geological Association of Canada, St. John's, 219–238.
Woo, J., Chough, S.K., and Han, Z., 2008, Chambers of *Epiphyton* thalli in microbial buildups, Zhangxia Formation (Middle Cambrian), Shandong Province, China. Palaios, 23, 55–64.
Woo, J., 2009, The Middle Cambrian Zhangxia Formation, Shandong Province, China: Depositional Environments and Microbial Sedimentation, Ph.D. thesis, Seoul National University, Seoul, 243 p.
Woo, J. and Chough, S.K., 2010, Growth patterns of the Cambrian microbialite: Phototropism and speciation of *Epiphyton*. Sedimentary Geology, 229, 1–8.

Manuscript received October 6, 2011
Manuscript accepted June 21, 2012